Quantum critical phenomena in a compressible displacive ferroelectric

Matthew J. Coak[a,1], Charles R. S. Haines[a,1], Cheng Liu[a], Stephen E. Rowley[a,b], Gilbert G. Lonzarich[a], and Siddharth S. Saxena[a,c,1]

[a]Cavendish Laboratory, Cambridge University, Cambridge CB3 0HE, United Kingdom; [b]Centro Brasileiro de Pesquisas Fisicas, Rio de Janeiro 22290-180, Brazil; and [c]National University of Science and Technology (NUST) "MISiS (Moscow Institute of Steel and Alloys)," Moscow 119049, Russia

Edited by Zachary Fisk, University of California, Irvine, CA, and approved April 16, 2020 (received for review December 21, 2019)

The dielectric and magnetic polarizations of quantum paraelectrics and paramagnetic materials have in many cases been found to initially increase with increasing thermal disorder and hence, exhibit peaks as a function of temperature. A quantitative description of these examples of "order-by-disorder" phenomena has remained elusive in nearly ferromagnetic metals and in dielectrics on the border of displacive ferroelectric transitions. Here, we present an experimental study of the evolution of the dielectric susceptibility peak as a function of pressure in the nearly ferroelectric material, strontium titanate, which reveals that the peak position collapses toward absolute zero as the ferroelectric quantum critical point is approached. We show that this behavior can be described in detail without the use of adjustable parameters in terms of the Larkin–Khmelnitskii–Shneerson–Rechester (LKSR) theory, first introduced nearly 50 y ago, of the hybridization of polar and acoustic modes in quantum paraelectrics, in contrast to alternative models that have been proposed. Our study allows us to construct a detailed temperature–pressure phase diagram of a material on the border of a ferroelectric quantum critical point comprising ferroelectric, quantum critical paraelectric, and hybridized polar-acoustic regimes. Furthermore, at the lowest temperatures, below the susceptibility maximum, we observe a regime characterized by a linear temperature dependence of the inverse susceptibility that differs sharply from the quartic temperature dependence predicted by the LKSR theory. We find that this non-LKSR low-temperature regime cannot be accounted for in terms of any detailed model reported in the literature, and its interpretation poses an empirical and conceptual challenge.

quantum criticality | ferroelectricity | high pressure

The study of quantum phase transitions and quantum critical systems has led to the discovery of novel phases of matter and the introduction of novel conceptual frameworks for the description of emergent phenomena (1). A quantum phase transition reached by varying a tuning parameter such as lattice density or electronic band filling fraction is imagined to separate two or more low-temperature states with qualitatively different types of order. An example is a transition from a magnetically polarized to a paramagnetic state in a metal. In the Kondo lattice model, for instance, at sufficiently low temperature the paramagnetic state is described as a Fermi liquid in which the elementary excitations arise from the hybridization of conduction electron states and well-localized f-electron orbitals.

Another example involves a transition from a displacive ferroelectric state to an unpolarized or quantum paraelectric state in polar materials such as the perovskite oxides (2–21). In contrast to the case of the magnetic metals, the nature of the unpolarized state in incipient ferroelectrics remains in some respects an enigma, especially in the low-temperature regime. In the simplest model, the quantum paraelectric state is characterized by an activated form of the temperature dependence of the inverse dielectric susceptibility in which the activation temperature scale vanishes at a continuous quantum phase transition [i.e., at a quantum critical point (QCP)]. However, this picture has proved to be insufficient and in particular is contradicted by the observation of an anomalous temperature dependence—including a mysterious minimum—in the inverse susceptibility of $SrTiO_3$ and related incipient displacive ferroelectrics at low temperatures (15, 16, 19, 22), which theoretical works have attempted to describe (3, 12, 15).

The identification of the nature of the quantum paraelectric states in such materials has been a key objective of the present study. This is a part of a more general goal to characterize and understand the temperature–quantum tuning parameter phase diagram of quantum critical ferroelectrics.

The absence of free charge carriers (in undoped samples) was expected to lead to a simpler phase diagram than that observed near to quantum critical points in metals, in which quantum critical phenomena are in many interesting cases masked by the emergence of intervening phases. These include unconventional superconductivity and exotic textured phases, which are of great interest but stand in the way of understanding quantum critical behaviors in their simplest forms over wide ranges down to very low temperatures.

To characterize the temperature–quantum tuning parameter phase diagram in close detail and obtain a deeper understanding of the quantum paraelectric state, we have carried out measurements of the dielectric response over a wide range in temperature

Significance

We present an experimental and theoretical study of the dielectric function of strontium titanate that clarifies the nature of quantum critical phenomena in ferroelectrics and helps to open up opportunities for the study of exotic normal and superconducting states in polar materials including ferrolectrics, ferrielectrics, antiferroelectrics, and multiferroics. As evidence, we show a series of high-precision studies as a function of temperature and pressure that dramatically confirm the applicability of a theory of the quantum critical state in displacive ferroelectrics and of superconductivity in polar materials—anticipated more than 50 y ago—and find states in regimes where this model breaks down.

Author contributions: G.G.L. and S.S.S. designed research; M.J.C., C.R.S.H., and C.L. performed research; M.J.C., S.E.R., and G.G.L. analyzed data; and M.J.C., C.R.S.H., G.G.L., and S.S.S. wrote the paper.

The authors declare no competing interest.

This article is a PNAS Direct Submission.

Data deposition: All relevant data are available as a data archive from the University of Cambridge repository: https://doi.org/10.17863/CAM.51389.

[1]To whom correspondence may be addressed. Email: mjc253@cam.ac.uk, crsh2@cam.ac.uk, or sss21@cam.ac.uk.

This article contains supporting information online at https://www.pnas.org/lookup/suppl/doi:10.1073/pnas.1922151117/-/DCSupplemental.

and pressure with high precision. In particular, the identification of the low-temperature behavior of the relative dielectric constant, ε_r, or dielectric susceptibility, $\chi = \varepsilon_r - 1$, has benefited from measurements of relative changes of χ as small as a few parts per billion. We first mention briefly the results of some relevant previous studies of our chosen material and then present and discuss our findings.

$SrTiO_3$ is a well-studied incipient displacive ferroelectric (23), widely used as a dielectric in deposition techniques and thin-film interface devices (24) as well as recently in high-precision thermometry (25), and is remarkable for having an extremely high dielectric susceptibility at low temperatures. At high temperatures, a good fit to the classically predicted Curie–Weiss form of the dielectric susceptibility is observed, with an extrapolated Curie temperature around 35 K (26), but this temperature dependence changes below approximately 50 K in the quantum critical regime and no ferroelectric ordering occurs down to the lowest temperatures measured. In addition, substitution of oxygen-16 for the oxygen-18 isotope results in the material becoming ferroelectric, and varying the level of isotope substitution or applying pressure (to samples with sufficiently high oxygen-18 concentrations) tunes the Curie temperature T_c to zero (27, 28). Uniaxial tensile strain applied to $SrTiO_3$ again causes it to become ferroelectric and suggests a small negative critical pressure of magnitude of the order of 1 kbar (29). Measurements of the dielectric susceptibility under pressure (30–32) show a drastic suppression of the low-temperature dielectric response as pressure is increased, matching the trend seen in the oxygen isotope doping studies, which see a maximum in the size of χ at a substitution level of 36%, the same point where T_c tends to zero temperature. At this quantum critical point, the frequency of the polar transverse optical phonon mode responsible for the ferroelectric ordering approaches zero at the Brillouin zone center (29). Recent work (33) has shown that the magnitude of the dielectric loss peak at approximately 10 K, associated with quantum critical effects (34), is linked to the quantum critical point in agreement with results from oxygen-18 substituted $SrTiO_3$ (9). An open question in the field remains as to the quantum phase transition empirically not becoming first order as temperature is lowered and lifting the quantum criticality (35). Although it is reasonable to expect that a ferroelectric transition such as this would turn first order, there is overwhelming evidence that the system is indeed quantum critical. Further work in the field is needed to advance understanding on this apparent contradiction.

These and related studies, including those on superconductivity in doped $SrTiO_3$ (21, 36–50), shed light on the likely broad features of the temperature–quantum tuning parameter phase diagram of $SrTiO_3$. We now turn to our present findings that allow us to construct the detailed phase diagram, with hydrostatic pressure, that preserves the high degree of homogeneity of the starting material, as the chosen quantum tuning parameter. Importantly, our results enable us to identify the physical nature of the quantum paraelectric state at pressures above the critical pressure of the ferroelectric quantum critical point at low temperatures, and in particular below the ubiquitous peak in the dielectric susceptibility.

Results

Fig. 1 shows measurements of the dielectric susceptibility $\chi = \epsilon_r - 1$ of $SrTiO_3$ at ambient pressure and at increasing applied pressures. The ambient pressure data match the results of earlier work (15, 51) wherein the inverse susceptibility is linear at high temperatures matching the expected Curie–Weiss behavior, before crossing over to a quadratic power law dependence at lower temperatures attributed to quantum critical fluctuations. The low-temperature dielectric susceptibility reaches a maximum at approximately 2 K with a value of around 20,000 before falling at even lower temperatures. Observed as a minimum in the inverse susceptibility, this effect is resolved here in much clearer detail than in earlier studies (15, 28) and crucially is investigated as a function of pressure. In Fig. 1*B*, this minimum is seen to increase in depth with increasing pressure, and its position, marked with vertical lines, moves up in temperature.

Key features of the susceptibility are brought out in Fig. 2, which shows the pressure dependences of the $T \to 0$ K inverse susceptibility $\chi^{-1}(0)$, (main plot), the square of the position of the minimum T^* (*Upper Inset*), and the depth of the minimum $\Delta\chi^{-1}(T^*) = \chi^{-1}(0) - \chi^{-1}(T^*)$ (*Lower Inset*). All three curves extrapolate to 0 at the same critical pressure, $p_c = -0.7(1)$ kbar (i.e., at the ferroelectric quantum critical point) as

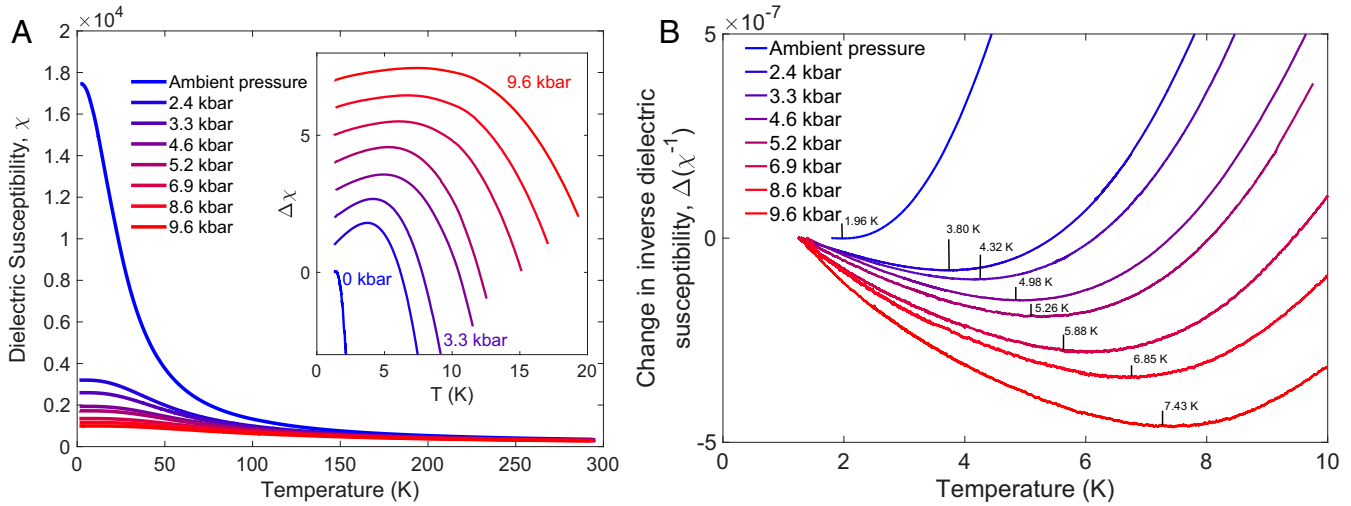

Fig. 1. (*A*) The dielectric susceptibility χ of $SrTiO_3$ plotted against temperature for applied pressures ranging from 0 (blue) to 9.6 (red) kbar. The magnitude of the dielectric susceptibility can be seen to be continuously reduced by the application of pressure. *Inset* shows the change in the low-temperature values of χ from their lowest-temperature values; curves are offset for clarity. Importantly, χ initially rises with temperature and exhibits a peak that increases in position and magnitude with increasing pressure. *B* shows the change in the inverse of χ from its lowest-temperature values for each pressure (typically 1.6 K), where the feature is now a clearly resolved minimum.

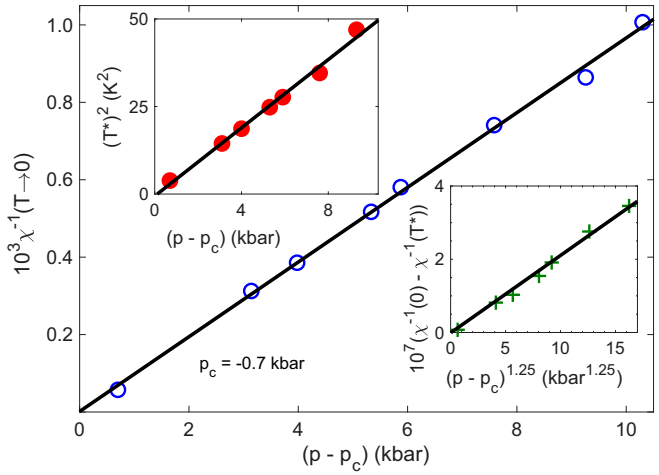

Fig. 2. The low-temperature inverse dielectric susceptibility $\chi^{-1}(0) = \chi^{-1}(T \to 0)$ as a function of applied pressure. We see that $\chi^{-1}(0)$ varies linearly with pressure and vanishes at the extrapolated critical pressure, p_c, of −0.7(1) kbar, defining the ferroelectric quantum critical point. *Lower Inset* and *Upper Inset* show the temperature dependences of the position of the minimum, T^*, and of the depth of the minimum, $\Delta\chi^{-1}(T^*)$, respectively. We see that the square of T^* is proportional to pressure and hence, also to $\chi^{-1}(0)$. This is characteristic of the model of coupled polar and nonpolar modes (i.e., the LKSR model) as described in the text. The solid lines in all three plots are guides to the eye.

suggested above. We see that $\chi^{-1}(0)$ varies linearly with $(p - p_c)$, T^* varies as the square root of $(p - p_c)$, and $\Delta\chi^{-1}(T^*)$ varies as $(p - p_c)$ to a power slightly greater than unity.

The variation of $\chi^{-1}(T)$ above a scale $T_{QC} > T^*$, which vanishes along with T^* at p_c, is found to be quadratic, T^2, up to another scale T_{CL}, and is linear in the classical regime above T_{CL} (Fig. 3 and *SI Appendix*). Pressure narrows the temperature window of the T^2 quantum critical regime between T_{QC} and T_{CL} while widening that below T_{QC}, including the interesting regime below T^*. *SI Appendix* and references therein have the error analysis and a full discussion of the fitting processes used in defining T_{QC} and T_{CL}. Combining the data for the pressure-dependent temperatures of the low-temperature minimum, T^* (Figs. 1 and 2, *Upper Inset*), and the cross-over temperatures from quantum paraelectric to quantum critical and from quantum critical to classical regimes, T_{QC} and T_{CL}, respectively, with previous data on $SrTi^{18}O_3$ (28) that yield the Curie (critical) temperature, T_c, under pressure allows a full mapping of the temperature–pressure phase diagram of $SrTiO_3$, which is shown in Fig. 3. The single ferroelectric quantum critical point at p_c is shown to be the origin of both the T^2 region of quantum critical behavior and seemingly, the energy scale of the minimum feature T^*—suggesting that this effect emanates from the QCP.

Discussion

The main features of this phase diagram are consistent with the predictions of a three-dimensional self-consistent Gaussian mean field model, also known as the self-consistent phonon model (e.g., ref. 15 and references therein), which assumes that $\chi^{-1}(0)$ is an analytic function of $(p - p_c)$ (in analogy to the assumption of analyticity in the Landau theory of phase transitions at finite temperatures) and that the temperature dependence $\chi^{-1}(T)$ is due to the thermal excitation of polar transverse optical modes whose gap, Δ, vanishes at the quantum critical point. The contribution of each mode depends on the inverse of their wavevector so that in three dimensions at the quantum critical point one expects a contribution to $\chi^{-1}(T)$ of the form $(1/T)T^3$, or T^2, far below the relevant Debye temperature, T_D, and of the form T above a temperature, T_{CL}, calculated numerically to be a sizeable fraction of T_D (15). Away from the quantum critical point where Δ is finite, the T^2 regime is cut off below a scale T_{QC} where the temperature dependence becomes exponentially weak as expected for activated phenomena. Since Δ^2 is expected to be proportional to $\chi^{-1}(0)$, which is proportional to $(p - p_c)$, we expect T_{QC} to be proportional to the square root of $(p - p_c)$, which is in keeping with observation (Fig. 3 and *SI Appendix*). Similar considerations lead us to expect T_c to also be proportional to the square root of $(p - p_c)$, which is consistent with previous studies in $SrTi^{18}O_3$. As shown previously for ambient pressure measurements, the self-consistent phonon model provides not only a qualitative but also, quantitative understanding of the above behavior in terms of independently measured model parameters.

However, the self-consistent phonon model in its simplest form fails to account for the low-temperature behavior presented here for $T < T^*$, which suggests that the quantum paraelectric state at low T is very different from the traditionally accepted gapped state with activated behavior [e.g., as described by the Barrett theory (52)]. In the remainder of the paper, we consider alternative possible descriptions of this state and attempt to clarify its physical nature.

We discuss first the role of the coupling of the electric polarization with the nonpolar lattice vibrations or acoustic phonons not included in the above self-consistent phonon model. As shown previously (3, 12, 15), this coupling can account for the existence of a minimum of the inverse susceptibility with values of T^* and depth $\Delta\chi^{-1}(T^*)$ that are consistent with zero-temperature model parameters inferred from other measurements. Extending measurements to include the effect of pressure tuning, however, sheds light on a particularly distinctive prediction of the model, namely that the square of T^* should vary linearly with $\chi^{-1}(0)$ and hence, vanish at the ferroelectric quantum critical point. This self-consistent phonon theory including polarization–acoustic phonon couplings is referred to here as

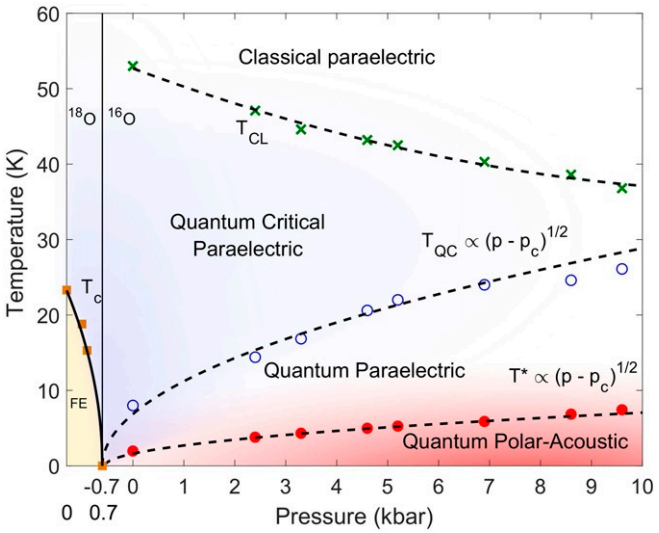

Fig. 3. Phase diagram for $SrTi^{16}O_3$ from −0.7 to 10 kbar (right side) and $SrTi^{18}O_3$ from 0 to 0.7 kbar (left side), overlaid to match up the positions of proposed QCPs. Closed circles give the positions of the low-temperature minimum, T^*, in χ^{-1} and open circles give the cross-over temperature, T_{QC}, from the quantum paraelectric to quantum critical regimes. Dashed lines give fits of $(p - p_c)^{1/2}$ behavior to both. Crosses show the cross-over temperature, T_{CL}, between quantum critical and classical Curie–Weiss behavior with a dashed guide to the eye. Squares and solid line show the ferroelectric (FE) Curie temperature, T_c, of $SrTi^{18}O_3$ taken from ref. 28.

the Larkin–Khemelnitskii–Shneerson–Rechester (LKSR) theory (3, 12, 15, 53, 54).

This prediction is strikingly supported by the data presented in the main plot and *Upper Inset* of Fig. 2, which show that both $(T^*)^2$ and $\chi^{-1}(0)$ vary linearly with $(p-p_c)$ and hence, are proportional to each other (*SI Appendix*, Fig S5). Moreover, as shown in *SI Appendix*, the absolute value of the slope of $(T^*)^2$ vs. $p-p_c$ or equivalently, $\chi^{-1}(0)$ is consistent in order of magnitude with independently measured model parameters—in particular, the results of the calculations for T^* vs. the square root of $(p-p_c)$ are shown in Fig. 4. Thus, at the critical pressure, p_c, $\chi^{-1}(T)$ has no minimum and is predicted to vary as the square of the temperature down to the lowest temperatures. For our model parameters, the transition to the ferroelectric state is expected to be essentially continuous at low temperatures, despite the polarization–acoustic phonons coupling (electrostriction) that is often expected to lead to first-order transitions. This prediction seems to be in keeping with measurements to date in isotopically, chemically, pressure-, and strain-tuned samples of $SrTiO_3$.

The LKSR model also predicts that the depth $\Delta\chi^{-1}(T^*)$ of the minimum should scale as $\chi^{-1}(0)$, which is partly supported from a comparison of the main plot and *Lower Inset* of Fig. 2. More importantly, the polarization–acoustic phonon coupling model (3, 12, 15) predicts that $\chi^{-1}(T)$ should vary as $(-T^4)$ well below the inverse susceptibility minimum, which is in sharp disagreement with the negative quasilinear dependence observed down to the lowest temperatures investigated (22). The breakdown of the distinctive $(-T^4)$ prediction of the model is particularly striking at high pressures where temperature ranges up to two orders of magnitude below T^* can readily be accessed, and the systematic variation of the slope and extent of the quasilinear term with $p-p_c$ are suggestive of an intrinsic phenomenon in some way connected with the quantum critical point.

This dramatic departure from the prediction of the LKSR model leads us to consider alternative explanations for the susceptibility minimum. One such alternative explanation involves the combined effects of long-range dipolar interactions between elementary dipoles and the short-range coupling of the polarization

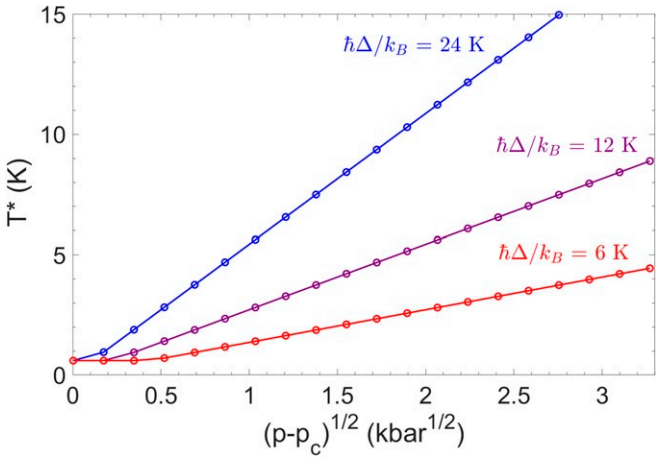

Fig. 4. Calculated pressure dependence of the temperature T^* of the minimum of the inverse susceptibility. Predictions of the self-consistent phonon model including the electrostrictive coupling (*SI Appendix*, Eqs. **S1–S5**) for T^* vs. $(p-p_c)^{1/2}$ of the inverse susceptibility vs. temperature for three values of the low-temperature and zero-pressure gap $\hbar\Delta/k_B$= 24 K (blue), 12 K (purple), and 6 K (red) (*SI Appendix* has the definition and determinations of the model parameters). The square of T^* is proportional to the pressure change measured from the ferroelectric quantum critical point at p_c, in agreement with observation (Fig. 2).

modes (55) (the mode–mode coupling) that can be represented in terms of an effective Euclidean action in a quantum description. It was suggested that this can lead to a susceptibility minimum qualitatively as predicted in the polarization–phonon coupling model but crucially with a $(-T)$ rather than $(-T^4)$ temperature dependence of $\chi^{-1}(T)$ below T^*, qualitatively as observed.

However, on closer examination we find that this negative T-linear form only applies to a material such as $SrTiO_3$ at energy scales above that of the longitudinal polar optical frequencies—temperatures far above the observed T^* in our experiments. In the temperature range below of the order of 10 K, the dipole–dipole interaction model predicts an exponentially weak rather than a $(-T)$ temperature dependence of $\chi^{-1}(T)$, which is in sharp disagreement with observation. For this and other reasons, the dipole–dipole interaction model seems to be untenable at least for the case of $SrTiO_3$ and does not explain the pressure dependence of T^* and of the depth of the minimum. It is also unlikely to operate in other materials where the minimum has been observed, such as tris-sarcosine calcium chloride (TSSC), which have ultraweak, nearly neutral, dipoles (16). We note, however, that the dipole–dipole interaction in polar doped alkali halides, for example, can promote antiparallel alignment of dipoles at low temperatures. This does indeed lead to a downturn in the dielectric susceptibility with decreasing temperatures at sufficiently low temperatures in these order–disorder paraelectrics that differ strongly from the displacive paraelectrics being considered here (e.g., ref. 56).

Another alternative explanation involves a possible refinement of the LKSR model, which as already noted, predicts correctly the linear relationship between $(T^*)^2$ and $\chi^{-1}(0)$. The chief weakness of this model, namely the predicted $(-T^4)$ temperature dependence of $\chi^{-1}(T)$ below T^*, compared with the observed $(-T)$ form, might be corrected via the inclusion of a low density of quasistatic modes of the lattice that can be treated effectively by classical statistics. To account for the observed $(-T)$ temperature dependence, the concentration of such modes only needs to be minute (below parts per million), since the Debye temperature is much larger than T^*, and normally outside the detection range of most probes. For example, the contribution to the specific heat capacity would be a small and virtually undetectable constant offset. Interestingly, simple numerical checks show that the inclusion of such a low density of slow classical modes, along with the acoustic phonons, leaves the pressure dependence of T^*, which defines a stationary point expected to be relatively insensitive to perturbations, largely unchanged. This suggests that the observed $(-T)$ variation of $\chi^{-1}(T)$ is not inconsistent with the observed linear variation of $(T^*)^2$ vs. $\chi^{-1}(0)$. In contrast, however, the dependence of the depth $\Delta\chi^{-1}(T^*)$ on $\chi^{-1}(0)$ is noticeably affected by the low density of slow modes, and this too is qualitatively in keeping with observation (main plot and *Lower Inset* of Fig. 2 and *SI Appendix*).

We now speculate on one possible origin of the proposed quasistatic modes. The LKSR model discussed thus far takes into account only the coupling of the polarization to the lattice density or to the volume strain. It has been shown that the coupling to nonuniform strain can in principle give rise to long-range strain-mediated interactions between the polarization modes (i.e., long-range mode–mode coupling). These long-range interactions are capable of producing microdomain structures in the polarization field under certain conditions (17, 57), which may be expected to exhibit slow temporal fluctuations and correspondingly, classical behavior even at temperatures well below T^*. Independent evidence for the possible existence of inhomogeneities comes from a number of studies (58) and for example, from recent measurements of the thermal conductivity (59), which reveal a surprisingly short mean-free path of phonons even in the millikelvin temperature range and in high-purity

single crystals of $SrTiO_3$. These speculations notwithstanding, the breakdown of the LKSR model at temperatures below the inverse susceptibility minimum remains a mystery and potentially a major subject for future study.

We therefore conclude that the susceptibility minimum in $SrTiO_3$ can be understood largely in terms of the LKSR model. An alternative explanation for the susceptibility minimum in terms of the anharmonic effects of the long-range dipole–dipole interaction is found to be untenable at least for the case of $SrTiO_3$. Thus, we may describe the quantum paraelectric state below T^* as a state in which the polarization field and the nonpolar lattice field are strongly hybridized, with the emergence at still lower temperatures of a previously unknown regime characterized by a linear temperature dependence of the inverse susceptibility. This is in sharp contrast to the conventional picture in which a ferroelectric quantum phase transition separates a ferroelectric state from an unhybridized paraelectric state characterized by an activated form of the temperature dependence of the inverse susceptibility. We have presented experimental findings and in the traditional way, compared these findings with existing theoretical models. Our analysis does not allow us to claim that the LKSR model has been "proved" even for the description of the origin of the inverse susceptibility minimum, only that it is more realistic than other proposals.

Finally, we note that a minimum of the inverse of the order parameter susceptibility is also observed in metals on the border of ferromagnetic quantum critical points. It is possible that at least in some cases the origin of this minimum can also be attributed to the coupling of the fluctuations of the order parameter field and lattice strain or to effects of magnetostriction in place of the effects of electrostriction in the ferroelectric systems.

Methods

High-precision capacitance measurements were carried out on single-crystal samples of $SrTiO_3$ from Crystal GmbH with gold electrodes vacuum evaporated onto the surfaces in a parallel-plate capacitor geometry. Measurements under hydrostatic pressure conditions were made possible by the development, in collaboration with CamCool Research Ltd, of a piston-cylinder clamp cell with miniature-shielded coaxial cables running into the sample region and electrically isolated from the cell body. This eliminates stray capacitances from the wiring and allows picofarad capacitance signals to be measured with stabilities of up to 10^{-18} F, a few parts in a billion. The shield conductors of the coaxial cables were joined together at the sample position and at the measurement instrument in the standard two-point capacitance setup. The pressure-transmitting medium was Daphne Oil 7373, and pressure values, determined from the superconducting transition temperature of a tin manometer, were estimated with an accuracy of 0.5 kbar. An Andeen-Hagerling 2550A capacitance bridge was used, with an excitation amplitude voltage of 0.1 V at a fixed frequency of 1 kHz applied to the sample. The sample thickness, corresponding to capacitor plate separation, was 0.5 mm. Measurements were taken on a modified 1 K Dipper cryostat from ICE Oxford, allowing continuous stable temperature control down to 1.2 K. Typical heating or cooling rates were held at 0.01 K per minute to allow the large thermal mass of the pressure cell to thermally equilibrate; temperature errors are of the order 10 mK at low temperature. Typical results of our measurements are shown in Fig. 1 and in *SI Appendix*, Figs. S1–S3.

Data Availability. All relevant data are available as a data archive from the University of Cambridge repository: https://doi.org/10.17863/CAM.51389.

ACKNOWLEDGMENTS. We thank J. F. Scott, D. M. Jarvis, J. van Wezel, L. J. Spalek, S. E. Dutton, F. M. Grosche, P. A. C. Brown, and C. Morice for their help in the development and evolution of this project; and D. E. Khmelnitskii, E. Baggio Saitovitch, P. Chandra, P. Coleman, V. Martelli, C. Panagopoulos, J.-G. Park, G. P. Tsironis, H. Hamidov, V. Tripathi, and M. Ellerby for their helpful advice and discussions. We acknowledge support from Jesus and Trinity Colleges of the University of Cambridge; the Engineering and Physical Sciences Research Council; the Conselho Nacional das Fundações Estaduais de Amparo à Pesquisa Newton Fund; the Royal Society; Institute for High Technology KAZATOMPROM, Kazakhstan; and United Kingdom Research and Innovation Global Challenges Research Fund COMPASS Grant ES/P010849/1. G.G.L. acknowledges the support of the National Council for Scientific and Technological Development, Brazil/Science without Borders Program, Centro Brasileiro de Pesquisas Fisicas, Rio de Janeiro, Brazil. Part of the work was carried out with financial support from the Ministry of Education and Science of the Russian Federation in the framework of Increase Competitiveness Program of NUST MISiS K2-2017-024, implemented by a governmental decree dated March 16, 2013, Number 211.

1. S. Sachdev, *Quantum Phase Transitions* (Cambridge University Press, 2011).
2. A. B. Rechester, Contribution to the theory of second-order phase transitions at low temperatures. *Sov. J. Exp. Theor. Phys.* **33**, 423 (1971).
3. D. E. Khmel'nitskiĭ, V. L. Shneerson, Low-temperature displacement-type phase transition in crystals. *Sov. Phys. Solid State* **13**, 832–841 (1971).
4. D. E. Khmel'nitskiĭ, V. L. Shneerson, Phase transitions of the displacement type in crystals at very low temperatures. *Sov. J. Exp. Theor. Phys.* **37**, 164–170 (1973).
5. U. T. Höchli, L. A. Boatner, Quantum ferroelectricity in $K_{1-x}Na_xTaO_3$ and $KTa_{1-y}Nb_yO_3$. *Phys. Rev. B* **20**, 266–275 (1979).
6. J. G. Bednorz, K. A. Müller, $Sr_{1-x}Ca_xTiO_3$: An XY quantum ferroelectric with transition to randomness. *Phys. Rev. Lett.* **52**, 2289–2292 (1984).
7. O. E. Kvyatkovskii, Quantum effects in incipient and low-temperature ferroelectrics (a review). *Phys. Solid State* **43**, 1401–1419 (2001).
8. R. Roussev, A. J. Millis, Theory of the quantum paraelectric-ferroelectric transition. *Phys. Rev. B* **67**, 014105 (2003).
9. E. L. Venturini, G. A. Samara, M. Itoh, R. Wang, Pressure as a probe of the physics of ^{18}O-substituted $SrTiO_3$. *Phys. Rev. B* **69**, 184105 (2004).
10. H. Wu, W. Z. Shen, Dielectric and pyroelectric properties of $Ba_xSr_{1-x}TiO_3$: Quantum effect and phase transition. *Phys. Rev. B* **73**, 094115 (2006).
11. N. Das, S. G. Mishra, Fluctuations and criticality in quantum paraelectrics. *J. Phys. Condens. Matter* **21**, 095901 (2009).
12. L. Pálová, P. Chandra, P. Coleman, Quantum critical paraelectrics and the Casimir effect in time. *Phys. Rev. B* **79**, 075101 (2009).
13. S. E. Rowley, "Quantum phase transitions in ferroelectrics," PhD thesis, University of Cambridge, Cambridge, UK (2010).
14. S. E. Rowley *et al.*, Ferromagnetic and ferroelectric quantum phase transitions. *Phys. Status Solidi* **247**, 469–475 (2010).
15. S. E. Rowley *et al.*, Ferroelectric quantum criticality. *Nat. Phys.* **10**, 367–372 (2014).
16. S. E. Rowley *et al.*, Quantum criticality in a uniaxial organic ferroelectric. *J. Phys. Condens. Matter* **27**, 395901 (2015).
17. S. E. Rowley, G. G. Lonzarich, Ferroelectrics in a twist. *Nat. Phys.* **10**, 907–908 (2014).
18. S. Horiuchi *et al.*, Quantum ferroelectricity in charge-transfer complex crystals. *Nat. Commun.* **6**, 7469 (2015).
19. S. E. Rowley *et al.*, Uniaxial ferroelectric quantum criticality in multiferroic hexaferrites $BaFe_{12}O_{19}$ and $SrFe_{12}O_{19}$. *Sci. Rep.* **6**, 25724 (2016).
20. P. Chandra, G. G. Lonzarich, S. E. Rowley, J. F. Scott, Prospects and applications near ferroelectric quantum phase transitions: A key issues review. *Rep. Prog. Phys.* **80**, 112502 (2017).
21. C. W. Rischau *et al.*, A ferroelectric quantum phase transition inside the superconducting dome of $Sr_{1-x}Ca_xTiO_{3-\delta}$. *Nat. Phys.* **13**, 643–648 (2017).
22. M. J. Coak, "Quantum tuning and emergent phases in charge and spin ordered materials," PhD thesis, University of Cambridge, Cambridge, UK (2017).
23. M. E. Lines, A. M. Glass, *Principles and Applications of Ferroelectrics and Related Materials* (Oxford University Press, 1977).
24. W. A. Atkinson, P. Lafleur, A. Raslan, Influence of the ferroelectric quantum critical point on $SrTiO_3$ interfaces. *Phys. Rev. B* **95**, 054107 (2017).
25. C. Tinsman *et al.*, Probing the thermal Hall effect using miniature capacitive strontium titanate thermometry. *Appl. Phys. Lett.* **108**, 261905 (2016).
26. K. A. Müller, W. Berlinger, E. Tosatti, Indication for a novel phase in the quantum paraelectric regime of $SrTiO_3$. *Z. Phys. B Condens. Matter*, **84**, 277–283 (1991).
27. M. Itoh, R. Wang, Quantum ferroelectricity in $SrTiO_3$ induced by oxygen isotope exchange. *Appl. Phys. Lett.* **76**, 221–223 (2000).
28. R. Wang, N. Sakamoto, M. Itoh, Effects of pressure on the dielectric properties of $SrTi^{18}O_3$ and $SrTi^{16}O_3$ single crystals. *Phys. Rev. B* **62**, R3577–R3580 (2000).
29. H. Uwe, T. Sakudo, Stress-induced ferroelectricity and soft phonon modes in $SrTiO_3$. *Phys. Rev. B* **13**, 271–286 (1976).
30. E. Hegenbarth, C. Frenzel, The pressure dependence of the dielectric constants of $SrTiO_3$ and $Ba_{0.05}Sr_{0.95}TiO_3$ at low temperatures. *Cryogenics* **7**, 331–335 (1967).
31. C. Frenzel, E. Hegenbarth, The influence of hydrostatic pressure on the field-induced dielectric constant maxima of $SrTiO_3$. *Phys. Stat. Sol.*, **23**, 517–521 (1974).
32. B. Pietrass, E. Hegenbarth, The influence of pressure on phase transitions at low temperatures: $SrTiO_3$ and $(Ba_xSr_{1-x})TiO_3$. *J. Low Temp. Phys.* **7**, 201–209 (1972).
33. M. J. Coak *et al.*, Dielectric response of quantum critical ferroelectric as a function of pressure. *Sci. Rep.* **8**, 14936 (2018).
34. R. Viana, P. Lunkenheimer, J. Hemberger, R. Böhmer, A. Loidl, Dielectric spectroscopy in $SrTiO_3$. *Phys. Rev. B* **50**, 601–604 (1994).
35. P. Chandra, P. Coleman, M. A. Continentino, G. G. Lonzarich, Quantum annealed criticality. arXiv:1805.11771 (30 May 2018).
36. J. F. Schooley, W. R. Hosler, M. L. Cohen, Superconductivity in semiconducting $SrTiO_3$. *Phys. Rev. Lett.* **12**, 474–475 (1964).
37. D van der Marel, J. L. M. van Mechelen, I. I. Mazin, Common fermi-liquid origin of T^2 resistivity and superconductivity in n-type $SrTiO_3$. *Phys. Rev. B* **84**, 205111 (2011).

38. J. F. Scott, E. K. H. Salje, M. A. Carpenter, Domain wall damping and elastic softening in $SrTiO_3$: Evidence for polar twin walls. *Phys. Rev. Lett.* **109**, 187601 (2012).
39. A. Lopez-Bezanilla, P. Ganesh, P. B. Littlewood, Research update: Plentiful magnetic moments in oxygen deficient $SrTiO_3$. *APL. Mater.* **3**, 100701 (2015).
40. S. E. Rowley *et al.*, Superconductivity in the vicinity of a ferroelectric quantum phase transition. arXiv:1801.08121v2 (24 January 2018).
41. X. Lin, Z. Zhu, B. Fauqué, K. Behnia, Fermi surface of the most dilute superconductor. *Phys. Rev. X* **3**, 021002 (2013).
42. K. Ueno *et al.*, Electric-field-induced superconductivity in an insulator. *Nat. Mater.* **7**, 855–858 (2008).
43. R. M. Fernandes, J. T. Haraldsen, P. Wölfle, A. V. Balatsky, Two-band superconductivity in doped $SrTiO_3$ films and interfaces. *Phys. Rev. B* **87**, 014510 (2013).
44. S. N. Klimin, J. Tempere, J. T. Devreese, D. van der Marel, Interface superconductivity in $LaAlO_3$-$SrTiO_3$ heterostructures. *Phys. Rev. B* **89**, 184514 (2014).
45. X. Lin *et al.*, Critical doping for the onset of a two-band superconducting ground state in $SrTiO_{3-\delta}$. *Phys. Rev. Lett.* **112**, 207002 (2014).
46. J. M. Edge, Y. Kedem, U. Aschauer, N. A. Spaldin, A. V. Balatsky, Quantum critical origin of the superconducting dome in $SrTiO_3$. *Phys. Rev. Lett.*, **115**, 247002 (2015).
47. J. Ruhman, P. A. Lee, Superconductivity at very low density: The case of strontium titanate. *Phys. Rev. B* **94**, 224515 (2016).
48. A. V. Chubukov, I. Eremin, D. V. Efremov, Superconductivity versus bound-state formation in a two-band superconductor with small Fermi energy: Applications to Fe pnictides/chalcogenides and doped $SrTiO_3$. *Phys. Rev. B* **93**, 174516 (2016).
49. L. P. Gor'kov, Phonon mechanism in the most dilute superconductor n-type $SrTiO_3$. *Proc. Natl. Acad. Sci. U.S.A.* **113**, 4646–4651 (2016).
50. A. Stucky *et al.*, Isotope effect in superconducting n-doped $SrTiO_3$. *Sci. Rep.* **6**, 37582 (2016).
51. K. A. Müller, H. Burkard, $SrTiO_3$: An intrinsic quantum paraelectric below 4 K. *Phys. Rev. B* **19**, 3593–3602 (1979).
52. J. H. Barrett, Dielectric constant in perovskite type crystals. *Phys. Rev.* **86**, 118–120 (1952).
53. A. I. Larkin, S. A. Pikin, Phase transitions of first order but nearly of second. *Sov. Phys. JETP-USS* **29**, 891–896 (1969).
54. A. I. Larkin, D. E. Khmel'nitskiĭ, Phase transition in uniaxial ferroelectrics. *Sov. Phys. JETP-USSR* **29**, 1123–1128, (1969).
55. G. J. Conduit, B. D. Simons, Theory of quantum paraelectrics and the metaelectric transition. *Phys. Rev. B* **81**, 024102 (2010).
56. W. N. Lawless, Impurity dipole interactions in alkali halides at low temperature. *Phys. Kondens. Mater.* **5**, 100–114 (1966).
57. R. T. Brierley, P. B. Littlewood, Domain wall fluctuations in ferroelectrics coupled to strain. *Phys. Rev. B* **89**, 184104 (2014).
58. E. K. H. Salje, O. Aktas, M. A. Carpenter, V. V. Laguta, J. F. Scott, Domains within domains and walls within walls: Evidence for polar domains in cryogenic $SrTiO_3$. *Phys. Rev. Lett.* **111**, 247603 (2013).
59. V. Martelli, J. L. Jiménez, M. Continentino, E. Baggio-Saitovitch, K. Behnia, Thermal transport and phonon hydrodynamics in strontium titanate. *Phys. Rev. Lett.* **120**, 125901 (2018).